Research Square

Preprints are preliminary reports that have not undergone peer review.
They should not be considered conclusive, used to inform clinical practice,
or referenced by the media as validated information.

Elucidating conformational preference of substituted azobenzenes with intramolecular symmetry-adapted perturbation theory

Du Luu
Auburn University
Konrad Patkowski
patkowsk@auburn.edu

Auburn University

Research Article

Keywords:

Posted Date: November 24th, 2026

DOI: https://doi.org/10.21203/rs.3.rs-11695239/v1

License: This work is licensed under a Creative Commons Attribution 4.0 International License.
Read Full License

Additional Declarations: No competing interests reported.

Elucidating conformational preference of substituted azobenzenes with intramolecular symmetry-adapted perturbation theory[†]

Du Luu and Konrad Patkowski*

Department of Chemistry and Biochemistry, Auburn University, Auburn, AL 36849

E-mail: patkowsk@auburn.edu

[†]Dedicated to the memory of Professor Bogumił Jeziorski.

Abstract

The cis-trans energy difference in the azobenzene molecule, an important photochemical switch, can be modulated by incorporating substituent groups. In particular, aliphatic substituents act as dispersion energy donors, enhancing the nonbonded attraction between the two aromatic rings in the cis configuration. On the other hand, the trans isomer remains favored by its lack of geometric distortion, that is, there is a deformation energy penalty to form the cis structure. In this work, we investigate the energetic balance between deformation and nonbonded interaction for 15 unsubstituted and substituted azobenzenes with accurate ab initio calculations. To obtain reliable intramolecular interaction energies and their decomposition into dispersion and other physical effects, we employ the intramolecular symmetry-adapted perturbation theory (ISAPT) approach in the novel SIAO1 variant recently introduced by us. The deformation energy is computed by considering intermediate, auxiliary one-ring systems that preserve molecular deformation but involve little to no intramolecular interaction. The sum of the two effects is compared to the conformational cis-trans energy differences from the reference domain-based local pair natural orbital coupled-cluster calculations, DLPNO-CCSD(T). We observe a very good correlation with the reference data, indicating that the energetic balance of substituted azobenzenes can indeed be explained by the interplay of nonbonded interaction and molecular deformation.

Introduction

Symmetry-adapted perturbation theory (SAPT) as a method to compute and interpret weak noncovalent interaction energies is nearly 100 years old.[1] It took many studies and methodological developments to evolve SAPT into the robust general-purpose approach of today, with several successful variants and efficient computer implementations. Professor Bogumił Jeziorski had been the visionary and the leader who spearheaded nearly of these developments. To name just a few examples, Jeziorski, Kołos, Szalewicz, and Chałasiński formulated a general framework encompassing different *symmetry forcing* techniques in SAPT

and proposed the simplest one, the symmetrized Rayleigh-Schrödinger (SRS) theory, that has become the variant of choice for all practical applications.[2,3] Jeziorski, Korona, and several others (including the present author in his graduate school years) took the SAPT theory to very high orders to investigate the convergence properties of different perturbation expansions.[4–6] Jeziorski, Szalewicz, Moszyński, and others formulated the *many-body SAPT* approach and derived an extensive set of many-body SAPT corrections in a double perturbation theory that uses the Møller-Plesset formalism to capture intramolecular electron correlation.[7–9] However, Professor Jeziorski was also instrumental in the development of alternative methods to include intramolecular correlation from density functional theory (SAPT(DFT), with Misquitta and Szalewicz[10,11]) and coupled-cluster theory (SAPT(CC), with Korona[12,13]).

Our group has been contributing to the further development of SAPT capabilities and, more often than not, our work has been inspired by Professor Jeziorski's seminal contributions. A good example is the variational formulation of dispersion energy[14] by Jeziorski and van Hemert and the subsequent development of explicitly correlated dispersion by Jeziorski and Szalewicz,[15] which paved the way for the combination of SAPT dispersion and exchange-dispersion with the F12 explicitly correlated approach.[16–18] In another development, the direct approach to computing interaction-induced properties by Piszczatowski, Łach, and Jeziorski[19] formed the basis for the new SAPT-based theory of interaction-induced dipoles, propSAPT.[20,21]

SAPT remains an active area of research, with the different novel enhancements and representative applications collected in several recent reviews.[22–26] Beyond the classic case of a noncovalent interaction between two molecules, SAPT has been extended to treat interactions between intermolecular fragments,[27,28] intramolecular fragments,[29,30] three molecules and the three-body nonadditivity,[31,32] and molecules embedded in an environment;[33–35] see Ref. 26 for a review of those extensions. The present work focuses on the physically meaningful description of noncovalent intramolecular interactions, leveraging the recent improve-

ments to the intramolecular SAPT (ISAPT) approach of Ref. 30 to explain trends in the cis-trans isomerization energies of substituted azobenzenes.

The energetic quantification of noncovalent interactions within the same molecule is inherently non-unique, but several groups proposed practical approaches to compute nonbonded intramolecular effects within a SAPT-like framework. On one hand, one can cut appropriate covalent bonds and cap them with hydrogens to arrive at an intermolecular model with similar, but not the same, interaction as the intramolecular system.[36,37] On the other hand, a SAPT-like energy decomposition is possible without altering the molecule if one cleverly selects the zeroth-order Hamiltonian and the perturbation. In such a case, the molecule is partitioned into the noncovalently interacting fragments A and B and a linker C which is connected to A and B by single covalent bonds. From then on, one needs to identify a zeroth-order wavefunction where the effects of noncovalent interaction are removed (so that they can be later reinstated via perturbation theory) but the covalent interactions are fully accounted for. In the intraSAPT method of Refs. 29 and 38, this identification is performed using the Chemical Hamiltonian technique[39] to arrive at a non-Hermitian zeroth-order operator and a noninteracting wavefunction that is a single determinant and thus includes polarization and exchange effects together. In the alternative approach of Ref. 30, known simply as ISAPT, the zeroth-order wavefunction is a product of individual determinants for A and B (just like in standard intermolecular SAPT), but these determinants are computed including the effects of linker C via a Hartree-Fock embedding.[40] The latter approach is the most "SAPT-like" and its zeroth-order wavefunction can be used to compute all energy corrections of the lowest-level standard SAPT variant, SAPT0.[41] However, the original ISAPT formulation of Ref. 30 was not free from artifacts that limited its practical usefulness.

The performance of the A-C-B molecular fragmentation underlying ISAPT is sensitive to the detailed splitting of electron density at the interfragment boundaries. The occupied Hartree-Fock (HF) orbitals of the entire molecule are localized to fragments using the intrinsic bond orbital (IBO) approach[42] which, in addition to orbitals localized entirely within a

specific fragment, produces two doubly occupied IBOs that describe the interfragment bonds (it is assumed in the original ISAPT formulation, as well as in this work, that the (A,C) and (B,C) pairs of fragments are connected by one single bond each). In the method of Ref. 30, it was assumed that the electrons occupying those interfragment IBOs are assigned to the linker C, together with a (+1) charge from the neighboring A and B atoms to preserve electrical neutrality of each fragment. However, such an assignment, denoted ISAPT(C) from now on, is prone to generating artificial dipole moments at the interfragment boundaries even when the A-C and B-C bonds are nonpolar (for example, in hydrocarbon molecules). The reason for this artifact becomes clear if one focuses on the atom of A (or B) connected to C: within its own fragment, it is missing the two electrons on one of its hybrid orbitals (the one pointing towards C) and thus acquires a dipole moment. The unphysical dipoles have a minor effect on some fragmentation patterns (especially those with a large linker C, i.e., when A and B are far apart) but an absolutely dramatic effect on others (those with a small linker C) — the resulting ISAPT corrections often do not make physical sense. For example, in systems exhibiting an intramolecular hydrogen bond between A and B (such as 2,4-pentanediol), the energy of such an obviously favorable interaction was often found to be quite positive (repulsive), with a strongly positive electrostatic component which should be the driving force for the hydrogen bond formation rather than destabilizing it. As a result, the utility of the ISAPT(C) approach in elucidating intramolecular nonbonded interactions in chemically interesting systems has been severely limited.

The spurious dipole moments at the ISAPT interfragment boundaries can be substantially reduced by an appropriate reassignment of the electron pair occupying the linking orbital. The idea of such a reassignment is, in a sense, to undo the interfragment bond formation and decompose the doubly occupied link IBO into a pair of intrinsic hybrid orbitals (IHOs), reassigning one electron of the pair to each IHO, and each IHO to its own fragment.[43] The resulting modified densities and reduced density matrices of fragments A and B are then used in standard SAPT0 energy expressions (with small modifications to

the exchange part resulting from the fact that the fragments are now open-shell). There is more than one way to define the pair of IHOs combining to the link IBO, and in Ref. 43 we recommended an algorithm called ISAPT(SIAO1) (splitting of intrinsic atomic orbitals (IAOs), one iteration) where the link orbital was projected onto the space of IAOs[42] localized on a given fragment. The resulting ISAPT(SIAO1) algorithm was shown to lead to significantly reduced dipole moments of formally nonpolar fragments compared to the original ISAPT(C) approach, a stable basis set convergence, and ISAPT energy contributions that make physical sense for all model systems and fragmentation patterns tested. Therefore, ISAPT(SIAO1) is now available for practical applications and expected to provide novel physical insights into the nature of nonbonded intramolecular interactions, at least for systems where two noncovalently interacting groups A and B and their linker C can be clearly identified. This fragmentation pattern is somewhat limiting; at present, ISAPT can only compute the A-B nonbonded interactions, not the ones involving C or those intrinsic to one fragment (e.g., A-A). To quantify and decompose the entire nonbonded energy in a molecule, a different strategy is required, and our preliminary study indicates that a range separation of the Coulomb potential might be an appropriate tool for this purpose.[44]

In this work, we apply the ISAPT(SIAO1) formalism to provide insights into the relative stability of the cis- and trans- conformers of substituted azobenzenes. Azobenzene and its derivatives are molecules considered to be prototype photomodulable materials and molecular devices.[45–49] Azobenzene and its derivatives undergo an efficient and reversible trans $\rightarrow$ cis photoisomerization in response to external stimuli, such as light, electrons, and temperature. The photoisomerization occurs without secondary processes, making azobenzene a highly versatile molecular switch.[50–54] A broad range of molecular design strategies in azobenzene photochemistry, particularly through substitutions on the aromatic rings, enables the fine-tuning of its isomerization mechanism for diverse applications, including light-responsive polymers, photochemical control agents, optical memories and switches, photoactuators, nanodevices, and molecular machines.[53–63]

An azobenzene molecule in the gas phase exhibits two structures. The global minimum is the trans geometry, a C_{2h} planar configuration. The cis structure is a nonplanar, C_2 one.[51] The two structures can interconvert upon irradiation: the photoisomerization primarily involves two singlet excited states and has been extensively studied experimentally.[51] In addition, the thermal isomerization process slowly converts the cis structure into the more thermodynamically stable trans one. The two configurations of azobenzene, with and without substituents, and their lowest excitation energies have been subject of a large range of computational studies, primarily at the density functional theory (DFT) level, where the functionals, basis sets, and solvent treatments have been thoroughly benchmarked.[64] A notable early work beyond the DFT level was the MP2/cc-pVTZ optimization and frequency calculation followed by coupled-cluster (CC2 and CCSD) excitation energy calculations for both conformers of unsubstituted azobenzene.[65] The highest accuracy for the ground and first excited state of cis- and trans-azobenzene has likely been achieved in the quantum Monte Carlo study of Dubecký et al.,[66] while a newer work[67] was notable for extending the excitation energy calculation to a coupled-cluster level with triple excitations, CC3, showing improvement for states with a significant doubly excited character. However, to our knowledge, the substituted azobenzene molecules have not yet been investigated using accurate *ab initio* methods.

Adopting the cis structure requires some geometric strain and disallows π-electron delocalization throughout both rings and the azo bridge, so the trans structure is energetically favored. On the other hand, the cis arrangement brings the aromatic rings into closer proximity, resulting in favorable $\pi - \pi$ noncovalent interactions. While this effect alone is too small to overcome the deformation energy penalty in the cis structure, the favorable London dispersion interactions can be further enhanced by substituents, for example aliphatic ones. Therefore, the balance between the trans-favoring deformation and cis-favoring dispersion (and other nonbonded interactions) in substituted azobenzenes is worth investigating.

The quantity that this work aims to understand and physically interpret is the confor-

mational energy difference between the cis and trans structures. We compute the reference values of such energy differences using the domain-based local pair natural orbital variant of the coupled-cluster method with singles, doubles, and noniterative triples, DLPNO-CCSD(T).[68–70] The intramolecular dispersion and other noncovalent effects can be reliably quantified using the new ISAPT(SIAO1) approach[43] which is publicly available in the Psi4 software.[71] The deformation energy is harder to estimate rigorously, but we propose a family of intermediate systems with one aromatic ring that can exhibit deformation as their structure is altered, but do not possess the noncovalent interactions of the kind that stabilizes the cis azobenzenes. This splitting, while approximate, is expected to provide useful insights into the trends in relative stability as the substituents are changed. Finally, those trends are corroborated using a functional group SAPT (F-SAPT) difference analysis[28,72] from a further decomposition of the ISAPT energy terms into fragment-fragment contributions.

Methodology and computational details

We consider the cis and trans minimum structures of the unsubstituted azobenzene as well as its all-*meta* substituted derivatives.[73] Each benzene ring has two identical substituents in the two *meta* positions, and the substituents can be -H (e.g., none), methyl, ethyl, isopropyl, or tert-butyl. These substituents were employed as dispersion energy donors to study the importance of dispersion on the thermal isomerization rates.[73] The pairs of substituents on the two azobenzene rings can be different, allowing for nonsymmetric molecules. Throughout the text, the different substitution patterns will be denoted by (first ring substituent)AB(second ring substituent), e.g. MeABMe for all methyl substituents or AB*i*Pr for one unsubstituted ring and one isopropyl substituted ring. Note that the rings are equivalent, so that e.g. *i*PrAB is equivalent to AB*i*Pr, and we will follow the second notation, with the second ring substituent larger or equal to the first ring one.

We consider all possible pairs of substituents ranging from none to *t*Bu, giving rise to

15 cis and 15 trans structures. These geometries were optimized with density functional theory, using the B3LYP functional with the -D3(BJ) dispersion correction[74] and the aug-cc-pVDZ≡aDZ basis set. We observed that an alternative, where the geometries are optimized at the second-order Møller-Plesset perturbation theory (MP2) in the same aDZ basis, leads to cis structures with the rings placed significantly too close to one another due to the well known MP2 overestimation of the aromatic interactions.[75] All geometry optimizations were carried out with the Gaussian program.[76] The optimized cis and trans structures are illustrated in Figs. 1 and 2, respectively.

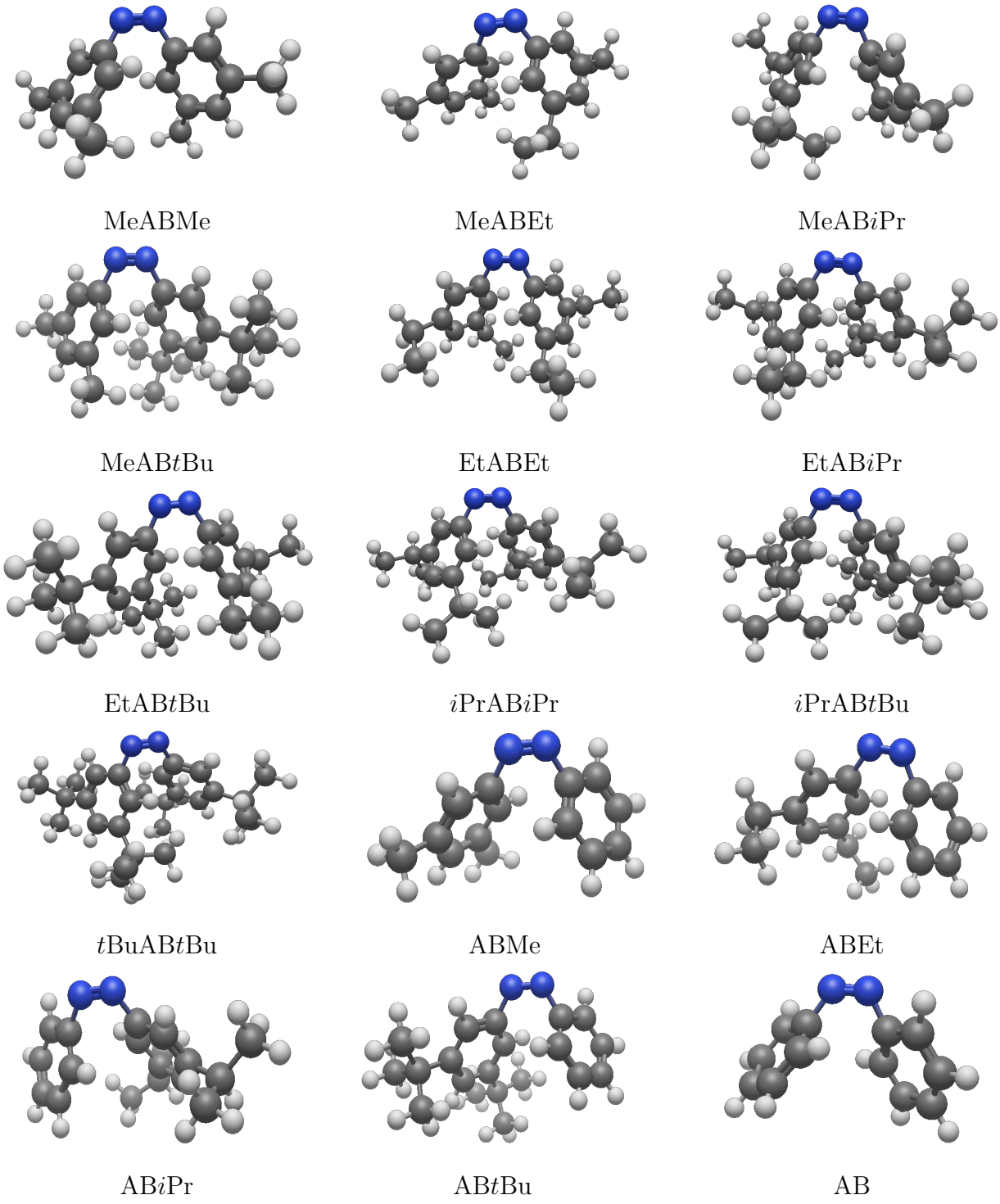

Figure 1: The geometric structures of the cis- all-meta alkyl substituted azobenzene molecules. The alkyl groups include methyl (Me), ethyl (Et), isopropyl (*i*Pr), and tert-butyl (*t*Bu).

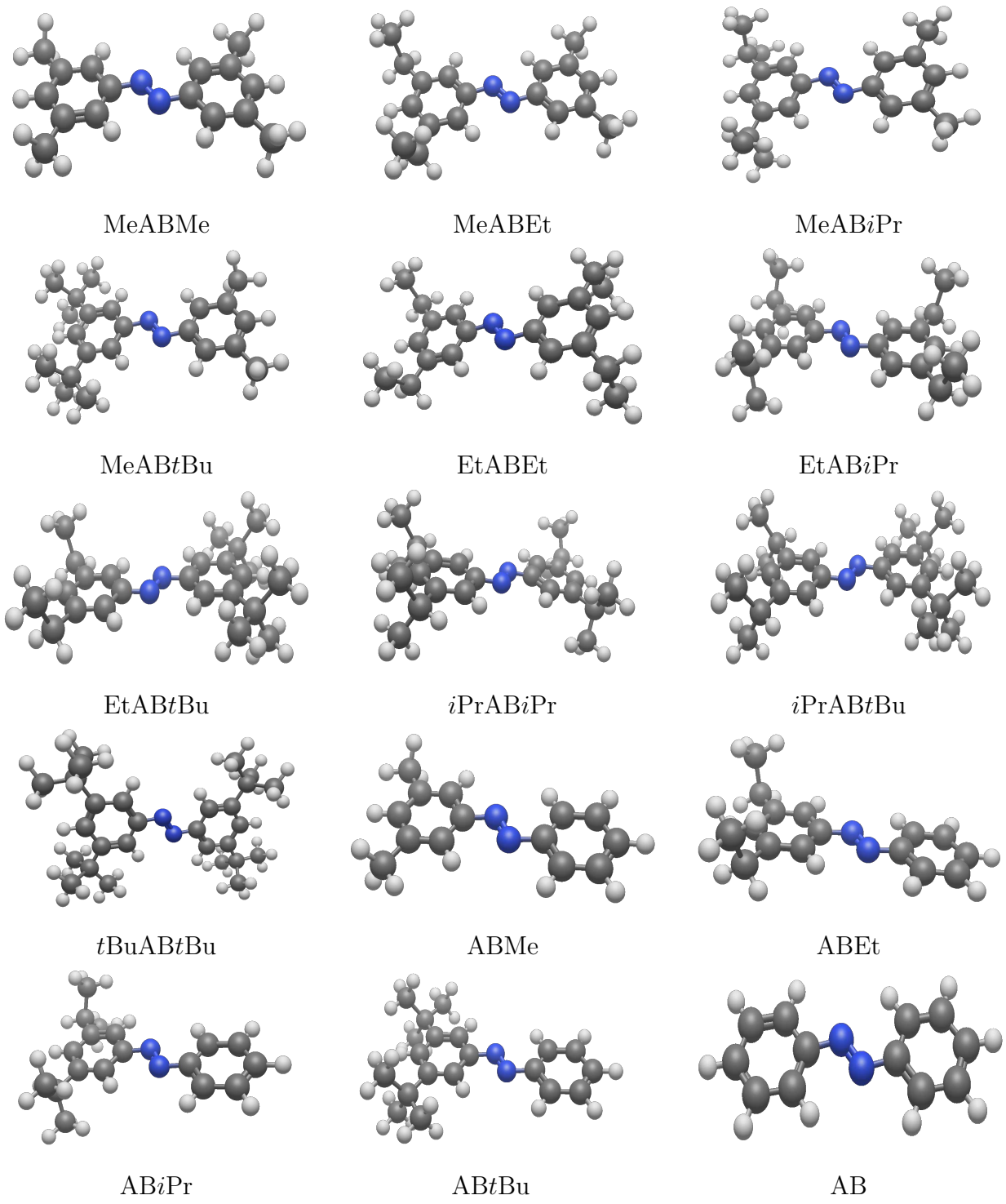

Figure 2: The geometric structures of the trans- all-meta alkyl substituted azobenzene molecules. The alkyl groups include methyl (Me), ethyl (Et), isopropyl (*i*Pr), and tert-butyl (*t*Bu).

The reference isomerization energies, that is, the differences $E_{\mathrm{cis}} - E_{\mathrm{trans}}$, were computed with the DLPNO-CCSD(T) level of theory and the aTZ basis set, using the ORCA program[77] and the `TightPNO` thresholds. The only exception were the two largest systems, *i*PrAB*t*Bu and *t*BuAB*t*Bu, for which the DLPNO-CCSD(T)/aTZ values would be too expensive to obtain; instead, those values were approximated by the common composite scheme, with all components still computed using the `TightPNO` thresholds:

$$E_{\mathrm{int}}^{\mathrm{DLPNO-CCSD(T)/aTZ}} \approx E_{\mathrm{int}}^{\mathrm{DLPNO-MP2/aTZ}} + \left(E_{\mathrm{int}}^{\mathrm{DLPNO-CCSD(T)/aDZ}} - E_{\mathrm{int}}^{\mathrm{DLPNO-MP2/aDZ}}\right) \quad (1)$$

We do not include the zero-point energy or thermal corrections in the reference energies since our decomposition into noncovalent interaction and deformation is also working on the non-zero-point corrected energies.

The ISAPT(SIAO1) calculations used the aTZ basis set and the PSI4 software.[71] The original ISAPT(C) variant was also computed for comparison. The noncovalent interaction energy in ISAPT is decomposed in a manner equivalent to the SAPT0 level of theory:[41]

$$E_{\mathrm{int}}^{\mathrm{ISAPT}} = E_{\mathrm{elst}}^{(10)} + E_{\mathrm{exch}}^{(10)} + E_{\mathrm{ind,resp}}^{(20)} + E_{\mathrm{exch-ind,resp}}^{(20)} + E_{\mathrm{disp}}^{(20)} + E_{\mathrm{exch-disp}}^{(20)} + \delta E_{\mathrm{int}}^{\mathrm{HF}} \quad (2)$$

In agreement with the SAPT literature, the two subscripts indicate the respective orders of perturbation theory with respect to interfragment interaction and intrafragment correlation (all SAPT0 corrections are of zeroth order with respect to the latter). The subscripts indicate the physical effect behind a given term, such as electrostatics, exchange repulsion, induction (polarization), the quenching of induction by exchange, London dispersion, and the quenching of dispersion by exchange.[78] The $\delta E_{\mathrm{int}}^{\mathrm{HF}}$ term corrects for higher-order induction and exchange-induction effects included in the supermolecular HF approach:

$$\delta E_{\mathrm{int}}^{\mathrm{HF}} = E_{\mathrm{int}}^{\mathrm{HF}} - E_{\mathrm{elst}}^{(10)} - E_{\mathrm{exch}}^{(10)} - E_{\mathrm{ind,resp}}^{(20)} - E_{\mathrm{exch-ind,resp}}^{(20)} \quad (3)$$

In standard intermolecular SAPT, the required HF interaction energy $E_{\rm int}^{\rm HF}$ is calculated as the difference $E_{\rm AB}^{\rm HF} - E_{\rm A}^{\rm HF} - E_{\rm B}^{\rm HF}$ between the HF energies of the complex and the monomers; in ISAPT, this recipe is slightly modified as

$$E_{\rm int}^{\rm HF} = E_{\rm ABC}^{\rm HF} - E_{\rm AC}^{\rm HF} - E_{\rm BC}^{\rm HF} + E_{\rm C}^{\rm HF}, \tag{4}$$

in other words, the interacting fragments and the supersystem are treated in the presence of the linker C, and then the energy of C is added to eliminate a double subtraction.[30] The shape of the substituted azobenzene molecule lends itself well to the ISAPT fragmentation. Each benzene ring, substituted or not, is taken as an interacting fragment A or B, and the linker C is defined as the –N=N– bridge.

We observed that, when the default IBO localization scheme was used in ISAPT without any further options, the resulting interaction energies were wrong for a subset of structures, breaking both the observed trends between systems and the consistency between the aDZ and aTZ basis. We suspect that those issues arose due to the difficulty of localizing the π clouds of those strongly conjugated systems, and observed that the issues are eliminated when the "stars" approach of Ref. 30 is used to enforce the localized orbitals to conform to a particular Kekulé structure on each aromatic ring. In the "stars" formalism, after the convergence of the initial IBO localization, a second iterative process is performed to maximize the localization function of Ref. 42 on a "starred" subset of carbon atoms, followed by another full IBO iterative localization. We found that if two "starred" atoms on each ring select a particular carbon-carbon bond 2–3 atoms away from the azo substituent, the IBO process consistently attains a slightly higher maximum of the localization function for all problematic systems, and that such a better localization leads to systematic and consistent ISAPT results. We do admit that the current need for such a manual (but consistent) adjustment to the localization process is not satisfactory, and we are exploring options to automate the process of guiding the IBO localization to its global maximum.

To provide a clearer picture of the substituent effects on the relative stability of conformers, we further split the ISAPT interaction energy terms into functional group contributions following the F-SAPT approach[28] (also called F-ISAPT in the intramolecular case). For this purpose, we split each noncovalently interacting fragment A (B) into three parts: the benzene ring A1 (B1) and two alkyl substituents A2,A3 (B2,B3), which might be just -H in the unsubstituted case. We follow this splitting by computing and displaying the differences in the respective F-SAPT interaction energy terms between the system of interest XABY (with substituents X and Y) and the unsubstituted azobenzene AB. In this way, the substituent effect on a particular interaction energy term is partitioned into its direct part (the difference between the interaction of substituents A2,A3,B2,B3 with the other fragment relative to the interaction of respective hydrogen atoms with the other fragment) and indirect part (the change in the interaction of the backbones, A1–B1, upon the substitution). An example of the F-SAPT partitioning of the trans-MeABEt system and the resulting intramolecular interaction energy decomposition is presented in Fig. 3. The F-SAPT difference analysis is a well established and useful method that takes advantage of likely error cancellations between the substituted and unsubstituted systems;[72] in the context of separating direct and indirect effects, it was used before e.g. in Ref. 79.

Deformation energy, the energetic penalty of the distortions in bond angles and lengths necessary to adopt the cis conformation, is the other contribution to the conformation energy difference separate from the nonbonded interaction energy. To estimate the deformation energy, we need to alter the system so that the A–B nonbonded interaction is removed, but the local geometry around each atom stays as close to the azobenzene system as possible. Therefore, we picked two intermediate systems resulting from a split of the azobenzene molecule into two separate noninteracting entities. The deformation effect is now estimated as the energy difference between the cis and trans configurations of the sum of noninteracting fragments, computed at the same DLPNO-CCSD(T)/aTZ level of theory as the reference isomerization energy. In the first variant, the separate fragments do not contain the azo

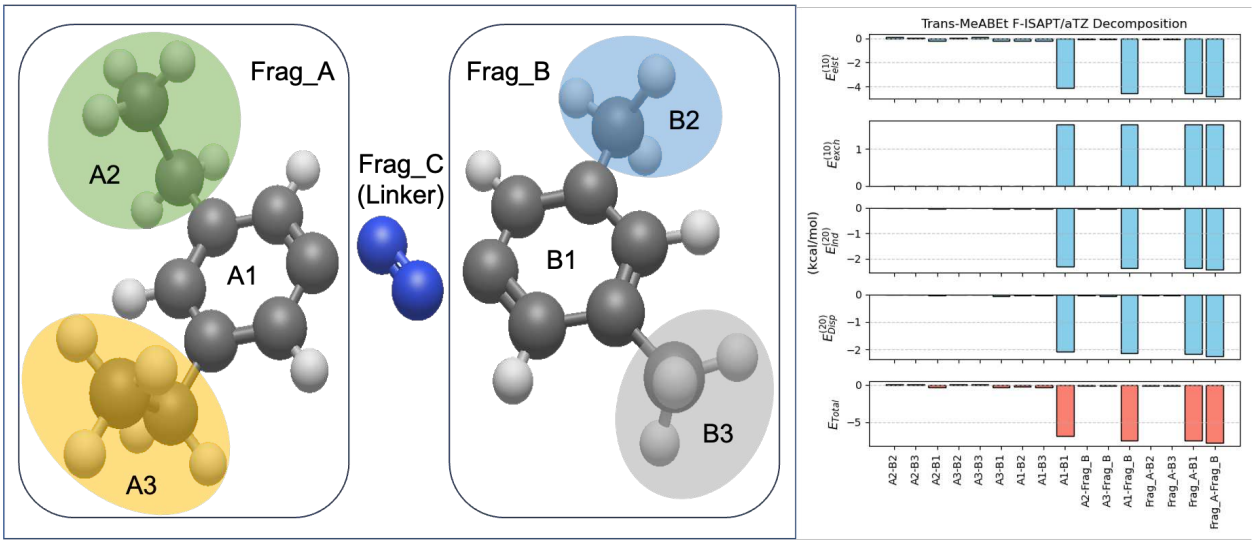

Figure 3: An example of the F-ISAPT fragmentation and intramolecular energy decomposition for the trans-MeABEt system. The left panel illustrates the geometric fragmentation of the trans-MeABEt molecule. It is separated into three fragments, denoted as Frag_A, Frag_B, and Frag_C. The missing bonds indicate the fragmentation. A1 and B1 are the benzene ring backbones of fragments A and B, respectively. A2 and A3 are the ethyl substituents in the fragment A. B2 and B3 are the methyl substituents in the fragment B. The right panel of the figure shows the F-ISAPT intramolecular energy decomposition (in kcal/mol) between the fragments A and B of trans-MeABEt, using the aTZ basis set.

group, so the corresponding conformational difference for the diazene molecule is added to cover the entire molecule:

$$\delta E_{\mathrm{def},1}(\mathrm{XABY}) \approx \delta E_{\mathrm{def}}(\mathrm{X_2Ph\text{-}H}) + \delta E_{\mathrm{def}}(\mathrm{H\text{-}PhY_2}) + \delta E_{\mathrm{def}}(\mathrm{H\text{-}N{=}N\text{-}H}) \tag{5}$$

In the second variant, the separate fragments each contain the azo group and capture the conformational energy differences at one end of that group:

$$\delta E_{\mathrm{def},2}(\mathrm{XABY}) \approx \delta E_{\mathrm{def}}(\mathrm{X_2Ph\text{-}N{=}N\text{-}H}) + \delta E_{\mathrm{def}}(\mathrm{H\text{-}N{=}N\text{-}PhY_2}) \tag{6}$$

In the calculation of all quantities on the r.h.s. of Eqs. (5) and (6), each δE_{def} represents the energy difference between the cis and trans geometries of a given fragment: those geometries are taken straight from the corresponding substituted azobenzene molecule. The

only variables that are optimized (at the MP2/aDZ level of theory) is the position of the capping hydrogen atom for each non-diazene fragment. For the HNNH molecule, only the two H-N bond lengths are optimized while the bond and dihedral angles are frozen in their corresponding azobenzene structure: obviously, a free optimization of the hydrogen positions would erase the cis-trans difference in this case.

Results and discussion

The first hint at the effects of an enhanced nonbonded interaction in the presence of dispersion energy donors is provided by the changes in the molecular geometry. As expected, the geometries of the trans isomers are highly consistent and planar, with the benzene rings parallel to one another (the interplane angle is up to 0.02 degree for symmetric systems and 0.7 degree for nonsymmetric systems), and all distances between two ring centers in the range (6.29,6.31) Å. However, the corresponding geometrical parameters for the cis isomers vary substantially with the substituents (by up to 12 degrees and 0.5 Å), as shown in Table 1. The increase in the substituent size generally decreases the inter-ring distance and decreases the angle between the two rings; thus, the dispersion-enhancing groups drive the aromatic rings closer and into a more stacked (less T-shaped) arrangement. This indicates that the attractive effect of the substituents as dispersion energy donors overpowers their repulsive effect due to increased size – we observe steric attraction rather than steric repulsion. The effects induced by the substituents on two azobenzene rings are cooperative and quite nonlinear: for example, the introduction of methyl groups on one ring in the unsubstituted AB system brings the ring centers closer by only 0.02 Å, but the same methyl group addition to AB*t*Bu (with tert-butyl groups on the other ring) reduces the inter-ring distance by 0.13 Å. A sufficient number of bulky substituents seems to saturate the balance between steric attraction and repulsion, and the differences between inter-ring distances and angles for the largest systems are fairly minor and not quite systematic. In fact, the shortest inter-ring

distance of 4.08 Å is in the *i*PrAB*t*Bu system, while the largest *t*BuAB*t*Bu one exhibits the second shortest distance of 4.18 Å. The smallest inter-ring angles of 50–51 degrees occur for systems with the bulky tert-butyl substituents on one ring and any substituents, even methyl, on the other ring.

Table 1: The angle θ between the planes of two aromatic rings (in degrees) and the distance d between the centers of these rings (in Å) for the cis isomers of substituted azobenzenes.

System	θ	d
AB	61.8	4.56
ABMe	61.1	4.54
ABEt	58.2	4.46
AB*i*Pr	57.8	4.46
AB*t*Bu	57.5	4.45
MeABMe	59.4	4.50
MeABEt	54.3	4.41
MeAB*i*Pr	54.2	4.41
MeAB*t*Bu	50.9	4.32
EtABEt	53.8	4.37
EtAB*i*Pr	53.5	4.39
EtAB*t*Bu	49.8	4.31
*i*PrAB*i*Pr	53.5	4.21
*i*PrAB*t*Bu	50.9	4.08
*t*BuAB*t*Bu	50.1	4.18

The reference isomerization energies (cis−trans differences) for all substituted azobenzenes, computed using DLPNO-CCSD(T), are collected in Fig. 4 for two basis sets, aDZ and aTZ. All these isomerization energies are positive, indicating that the trans structure is more stable on account of π conjugation and a lack of substantial deformation. However, the extent of the cis−trans energy difference decreases significantly with the size of the substituents, owing to an increasingly favorable intramolecular nonbonded interaction in the cis configuration. When going from the unsubstituted system AB all the way to *t*BuAB*t*Bu, the isomerization energy decreases from 10.0 to 2.3 kcal/mol in the aDZ basis, and from

11.4 to 6.2 kcal/mol in the aTZ basis. Thus, this range of substituents cannot make the cis configuration more energetically favorable than the trans one, but the set of four *t*Bu groups comes quite close.

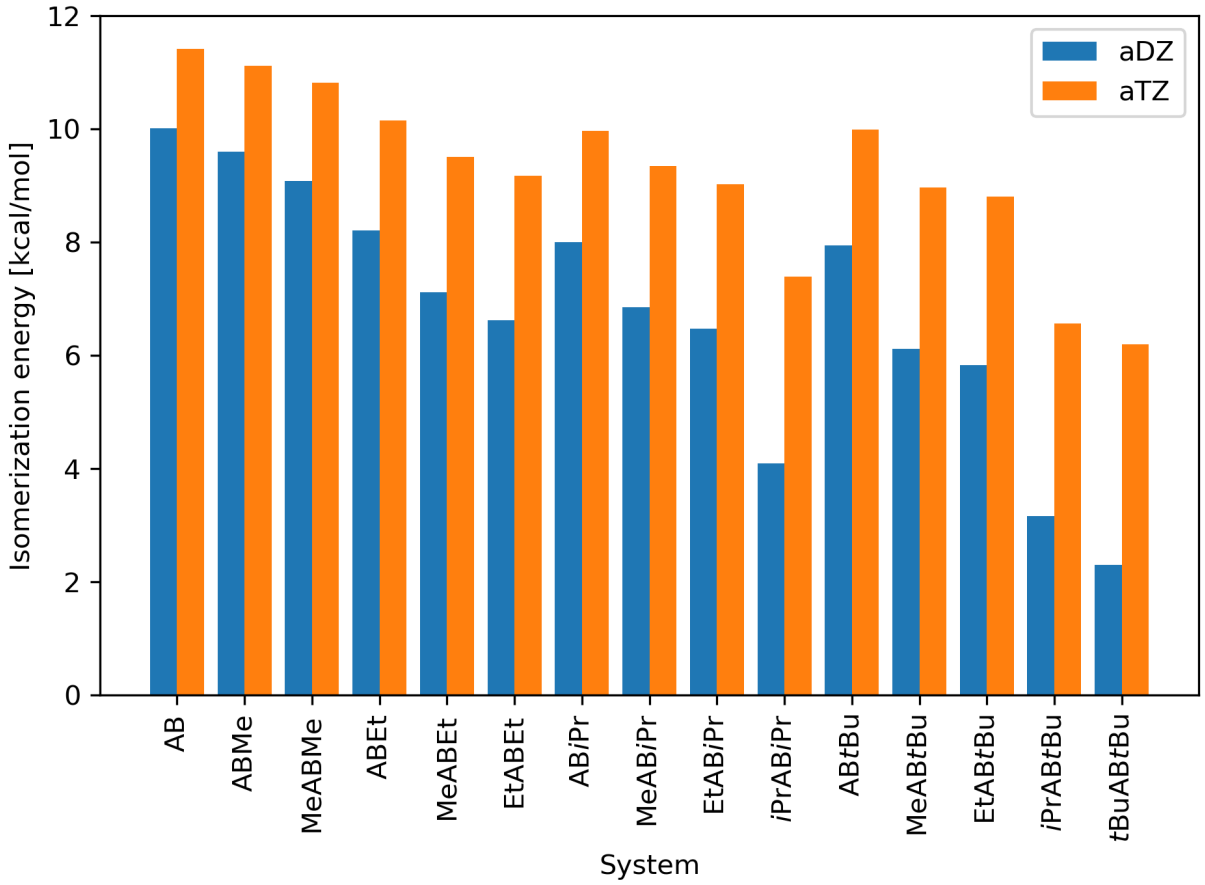

Figure 4: Isomerization energies for different substituted azobenzenes, computed as differences between the DLPNO-CCSD(T) energies of the cis and trans isomer. The data computed in two basis sets are shown.

The ISAPT(SIAO1) intramolecular interaction energy components, computed in the aTZ basis set, are presented in Fig. 5 for the cis configurations and Fig. 6 for the trans ones. The analogous ISAPT(C) results, with the original link orbital splitting algorithm of Ref. 30, are presented in the Supplementary Information: however, ISAPT(C) predicts repulsive total interaction energies for all cis systems, which is not physically justified as it has to be the nonbonded interaction that stabilizes the cis local minima on the potential energy surface.

We conclude that, once again, the insights from ISAPT(C) are not reliable and it is essential to use the modified ISAPT(SIAO1) algorithm from Ref. 43. With the latter algorithm, Fig. 5 shows an attractive nonbonded interaction between the two benzene rings in the cis arrangement that is systematically enhanced by adding larger and larger substituents. The increase in the size of the aliphatic group increases the strength of both the leading attractive component (dispersion), the second leading attractive term (electrostatics), and the leading repulsive contribution (first-order exchange). While those three SAPT components (and, to a smaller extent, the fourth component, induction, as well) follow the same trend, the total interaction energy becomes somewhat more attractive as the substituents increase, indicating that the growth in exchange repulsion does not fully make up for the growth in the dispersion and electrostatic attractions.

The results for the trans isomers, presented in Fig. 6, vary in a much smaller range than those for the cis isomers, and the overall ISAPT interaction energy terms are smaller in magnitude (which is expected since the aromatic rings are further apart). Unlike the primarily dispersion-bound character of the cis configurations, the nonbonded attraction in the trans systems is dominated by electrostatics. After that, the induction and dispersion components are of equal magnitude, and one of them is sufficient to offset the small exchange repulsion. The first-order exchange energy for the unsubstituted azobenzene is minimally negative. This might be some residual effect of the link bond redistribution even in the ISAPT(SIAO1) variant, however, the effect is too small to have practical consequences. Interestingly, all systems that have substituents on both rings (even MeABMe) exhibit stronger electrostatic attraction, exchange repulsion, and net nonbonded attraction than systems where at least one ring is unsubstituted (even AB*t*Bu). This can possibly be explained by the fact that the substituents extend out of the molecular plane, providing some three-dimensional density overlap that enhances all nonbonded contributions.

A finer-grained insight into the origins of intramolecular interactions in our systems can be provided by the F-SAPT decomposition of the ISAPT(SIAO1) data. In this decompo-

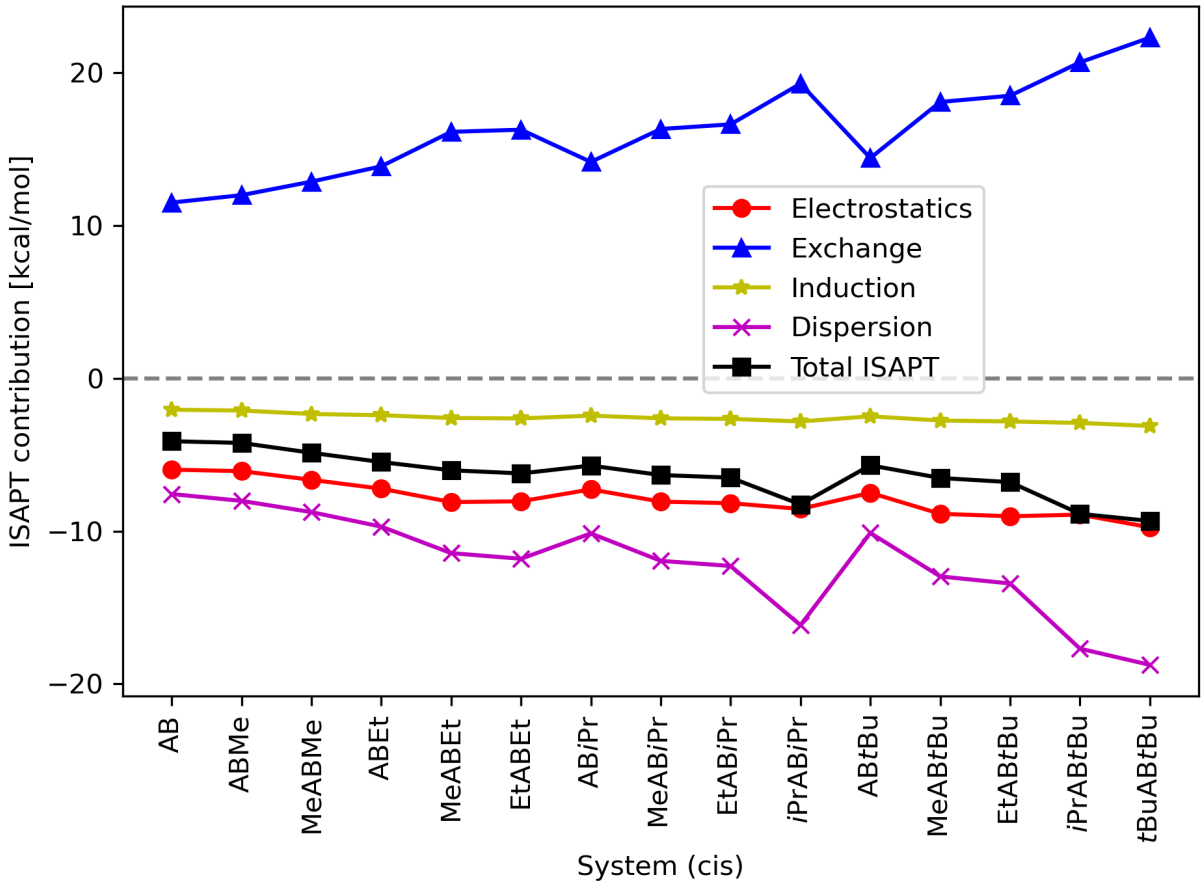

Figure 5: ISAPT(SIAO1)/aTZ intramolecular nonbonded energy contributions for the cis isomers of substituted azobenzenes.

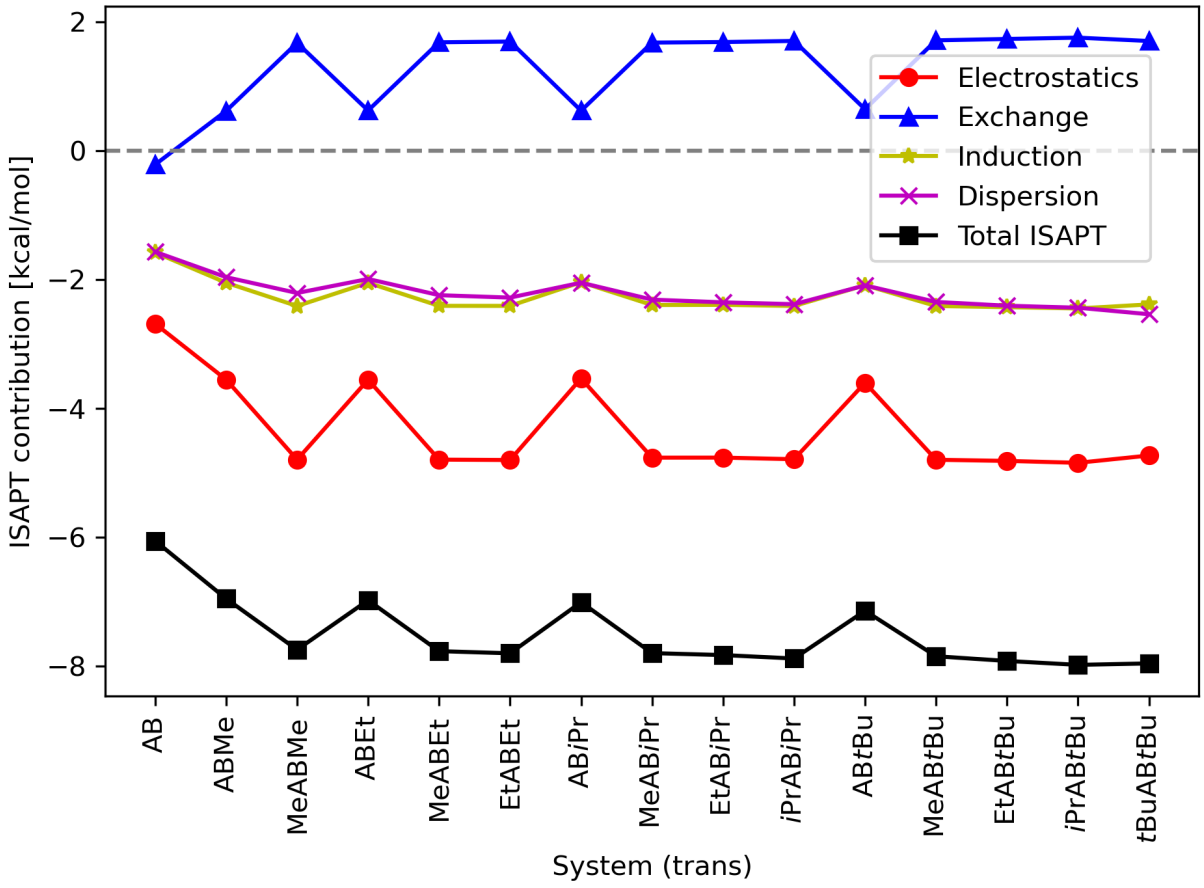

Figure 6: ISAPT(SIAO1)/aTZ intramolecular nonbonded energy contributions for the trans isomers of substituted azobenzenes.

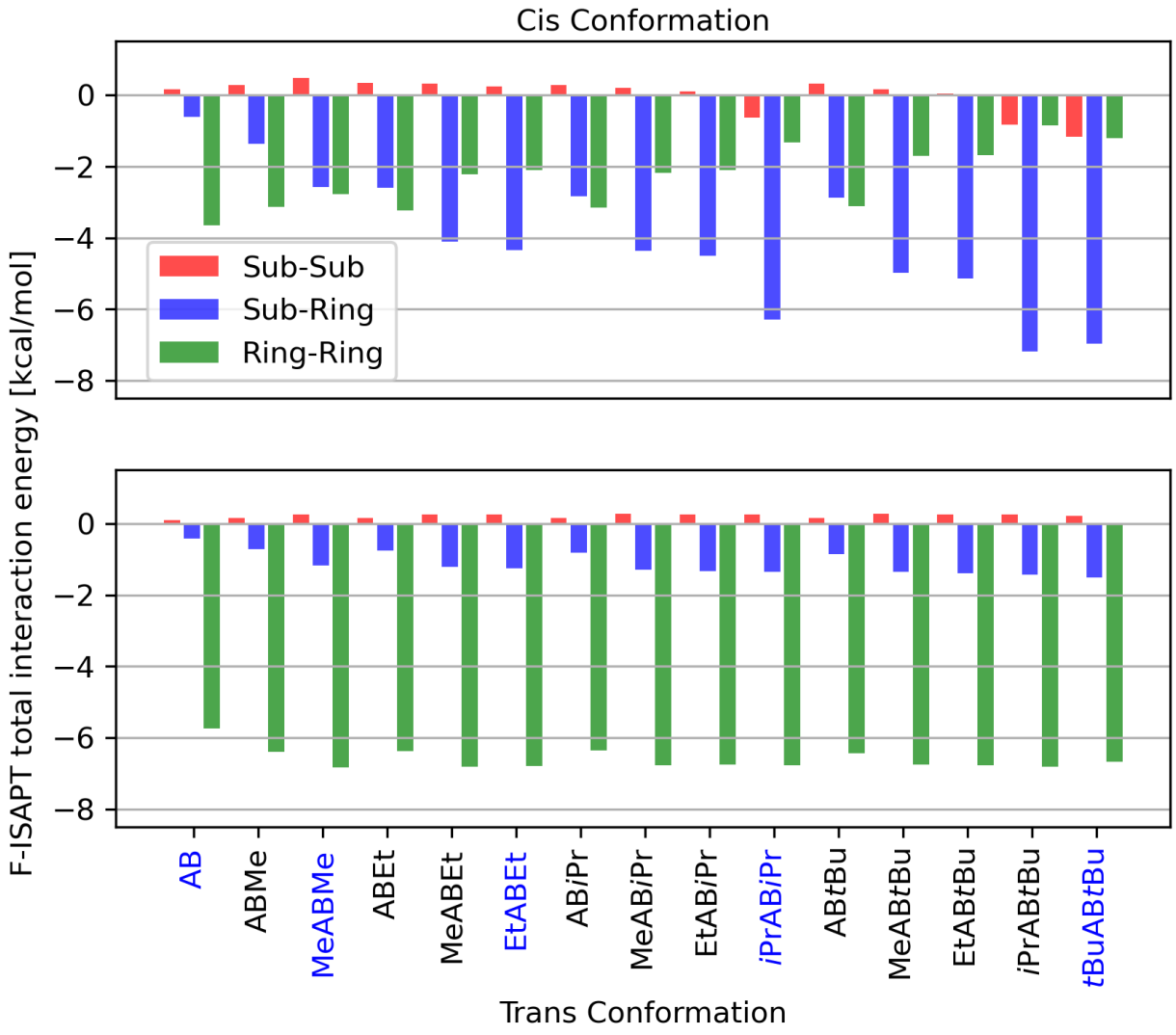

Figure 7: F-ISAPT(SIAO1)/aTZ total intramolecular nonbonded energy decomposition into substituent-substituent, ring-ring, and mixed substituent-ring contributions. The substituents are all in the meta positions and, in some systems, might amount to only a hydrogen atom.

sition, we separate the effects of substituents (all in meta positions) from those of the two benzene rings, leading to the substituent-substituent, ring-ring, and mixed substituent-ring interactions (each substituent can be either a hydrogen atom or an aliphatic group – see Fig. 3 for an illustrative example). The resulting F-ISAPT partitioning of the total interaction energies is presented in Fig. 7; the analogous partitionings for the individual ISAPT terms are presented in the Supplementary Information.

The first observation evident from Fig. 7 is that the nonbonded interaction energy is of very different origin in the trans and cis conformations of substituted azobenzenes. In the former case, the total interaction energy is strongly dominated by its ring-ring component, with only a secondary attractive contribution from the substituent-ring interactions and nearly negligible (and repulsive) substituent-substituent terms. Interestingly, the changes in the ring-ring and substituent-ring contributions track each other quite well, and the slightly weaker binding in the AB(Sub) complexes, where only one ring is substituted, can be attributed to both terms in similar proportions. In the cis case (the upper panel in Fig. 7), the nonbonded interaction is usually dominated by the mixed terms, except for the systems without a substituent on one ring and the MeABMe one: in the latter cases, the ring-ring term is more strongly attractive. For the most substituted complexes, the ring-ring contributions show less attraction but the mixed substituent-ring terms become much more favorable. The substituent-substituent interactions in the cis configurations can be both repulsive (for smaller substituents) and attractive, up to about 1 kcal/mol in magnitude for *i*PrAB*i*Pr, *i*PrAB*t*Bu, and *t*BuAB*t*Bu (that observed attractive character can be attributed almost exclusively to dispersion energy). A further examination of the individual F-ISAPT contributions, displayed in the Supplementary Information, shows that the dominant character of the substituent-ring terms for cis conformations is a result of a cancellation: the ring-ring terms dominate each of the four major SAPT components, but the attractive electrostatic, induction, and dispersion ring-ring energies get nearly cancelled by the repulsive exchange energy. This cancellation is much less complete for the substituent-ring terms, where the

repulsive exchange energy is overcome by the electrostatic energy alone, while the dispersion energy substantially enhances this type of binding.

For the subsequent analysis, we will combine the substituent-substituent and substituent-ring terms into a single contribution directly related to the substitution. On the other hand, the ring-ring terms will be termed indirect as they are only altered through the change in their electron densities in the presence of substituents. The direct and indirect substituent effects can now be quantified by the F-ISAPT difference analysis, in which each F-ISAPT contribution for a substituted system (Sub1)AB(Sub2) is computed relative to the unsubstituted AB baseline. The resulting F-ISAPT differences for each physical energy contribution (electrostatics, exchange, induction, dispersion, and total) and each substitution mode (direct, indirect) are collected in Figs. 8 and 9 for the cis and trans configurations, respectively.

The individual ISAPT components in Fig. 8 show that the direct and indirect effects amplify one another for the cis configurations except for the electrostatic energy for four systems including *i*PrAB*i*Pr and *i*PrAB*t*Bu. The primary source of the substituent effects on electrostatics and dispersion is the direct change between the interaction involving the substituent and the hydrogen atom it replaces. On the contrary, the indirect contribution dominates the exchange repulsion, although the direct term comes close for the most substituted systems. The induction contribution is very small and primarily indirect. Taking all ISAPT components together, the direct term alone overestimates the enhancement of the intramolecular attraction due to the substituents, and the repulsive indirect substitution effects cancel some of the enhancement.

The individual F-ISAPT contributions for the trans conformations of substituted azobenzene, Fig. 9, are overall much smaller (note the different energy scale relative to Fig. 8) and strongly dominated by the indirect contributions, with a small direct effect due to electrostatics plus some dispersion. The exchange effect is entirely indirect, as the substituents are too far apart in the trans conformations to exhibit any meaningful overlap. We see that the enhancement of intramolecular binding in the disubstituted trans isomers (Sub1)AB(Sub2)

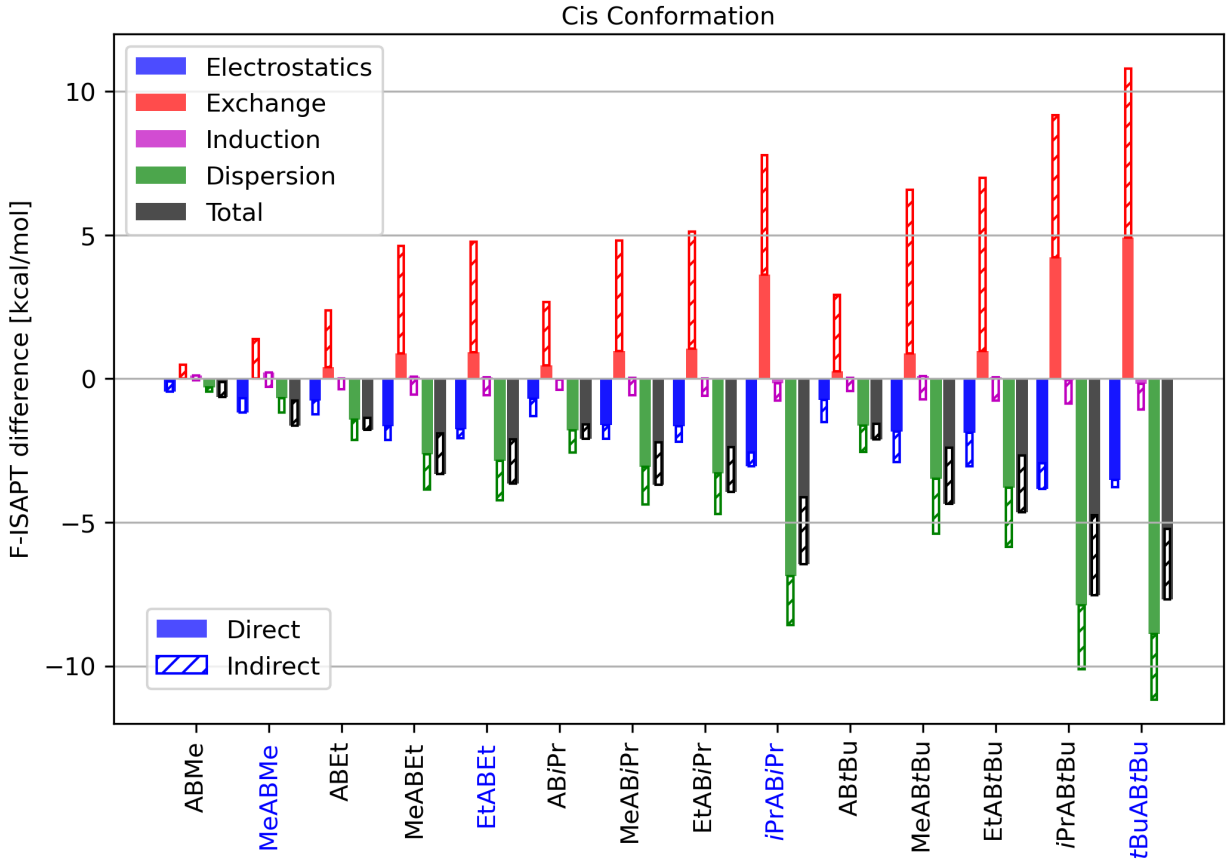

Figure 8: F-ISAPT(SIAO1)/aTZ difference analysis for the cis conformations of substituted azobenzenes, decomposing the intramolecular interaction energy in a substituted system relative to the unsubstituted AB one. Each SAPT contribution is split into the direct difference (solid bars), coming from the interactions between the substituent and the other fragment, and the indirect difference (hatched bars) resulting from the change in the interaction between the rings due to their altered electronic structure. The hatched bars are drawn narrower than the solid ones to visually distinguish the cases when the two effects amplify (for example, dispersion) or partially cancel one another (for example, total interaction energies).

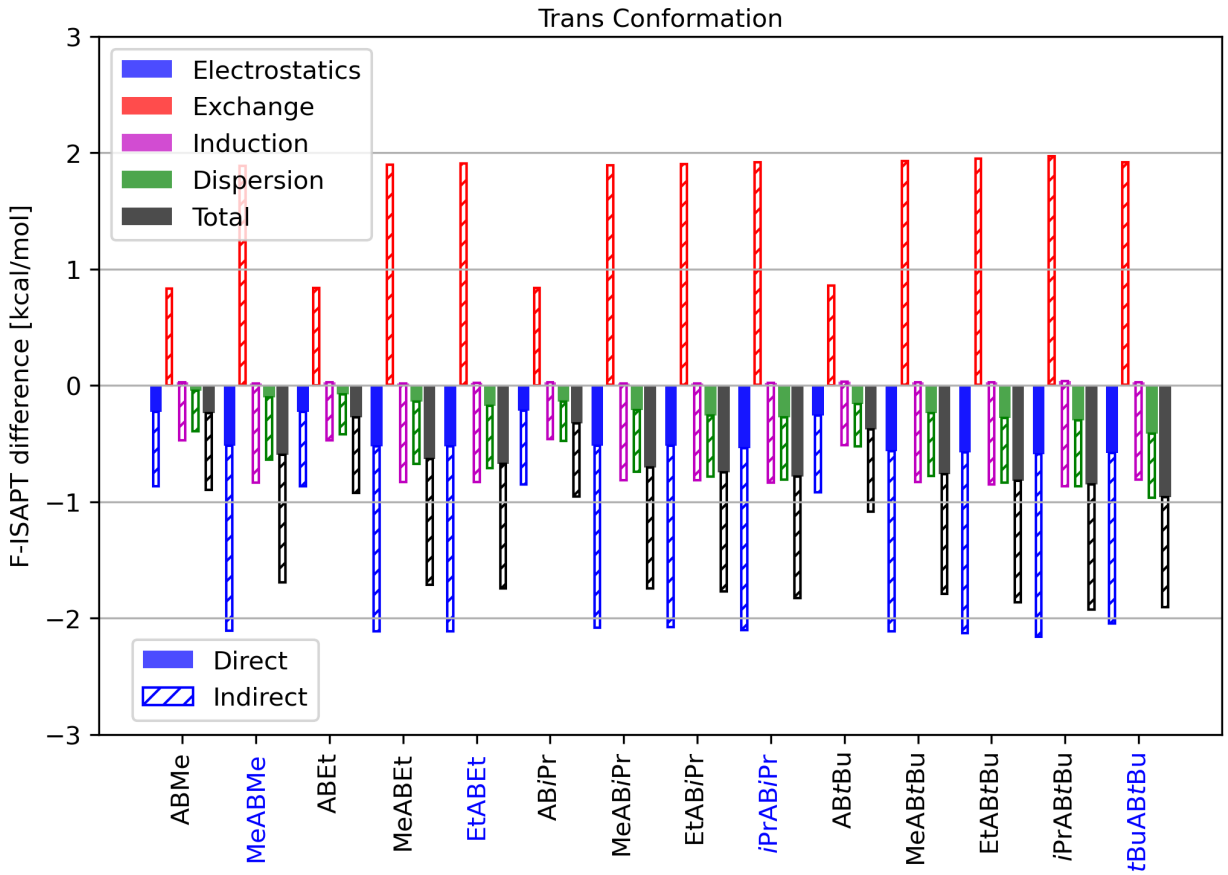

Figure 9: F-ISAPT(SIAO1)/aTZ difference analysis for the trans conformations of substituted azobenzenes, decomposing the intramolecular interaction energy in a substituted system relative to the unsubstituted AB one. Each SAPT contribution is split into the direct difference (solid bars), coming from the interactions between the substituent and the other fragment, and the indirect difference (hatched bars) resulting from the change in the interaction between the rings due to their altered electronic structure.

relative to the monosubstituted ones, AB(sub), arises due to the more attractive, and primarily indirect, electrostatic contribution. Apparently, the small difference in the electron redistribution between the nonpolar C-C bond and a nearly nonpolar C-H one is enough to provide some enhancement of the substituent effect on the electrostatic energy. The total interaction energy relative to the unsubstituted AB system remains nearly always dominated by the indirect contribution, but the direct effect is of similar magnitude for the largest, *t*BuAB*t*Bu system.

We have now completed a deep dive into the origins of the intramolecular nonbonded attraction and its changes upon substitution. For the final part, we want to pair the intramolecular interaction with an estimate of the monomer deformation effects to investigate if the cis-trans isomerization energy can be explained by the combination of the two. To this end, we added up the ISAPT(SIAO1)/aTZ nonbonded interaction energy difference between the cis and trans XABY conformations and the deformation energy estimate obtained from the DLPNO-CCSD(T)/aTZ energy differences for intermediate systems, as defined by Eqs. (5)–(6). The resulting sum of the nonbonded interaction and deformation effects is compared to the reference DLPNO-CCSD(T) (cis−trans) energy difference in Figs. 10 and 11 for the deformation estimates of Eq. (5) and Eq. (6), respectively. Quite reassuringly, both combined estimates of the interaction and deformation track the reference conformational energy differences well, with the R^2 coefficient of determination equal to 0.94 for Eq. (5) and 0.93 for Eq. (6). Furthermore, the first of these estimates is nearly parallel to the reference energy differences, with an 1.06 slope of the linear fit reported in Fig. 10. Thus, the combination of our nonbonded interaction and deformation estimates can successfully explain nearly the entire energy difference between the cis and trans substituted azobenzene conformations; the remaining effect of the order of 2 kcal/mol (the intercept in Fig. 10) is well within the expected range of accuracy for both the SAPT0-level interaction energy and the deformation energy estimate through Eq. (5). The deformation energy estimate of Eq. (6) and Fig. 11 performs worse, with a 0.71 slope of the linear fit. This might indicate

that Eq. (6) might suffer from some partial double counting of the deformation around the azo group. However, such double counting is far from complete: if one subtracts the HNNH conformational energy difference from Eq. (6) to try to account for full double counting, the correlation to reference data is lost ($R^2 = 0.45$).

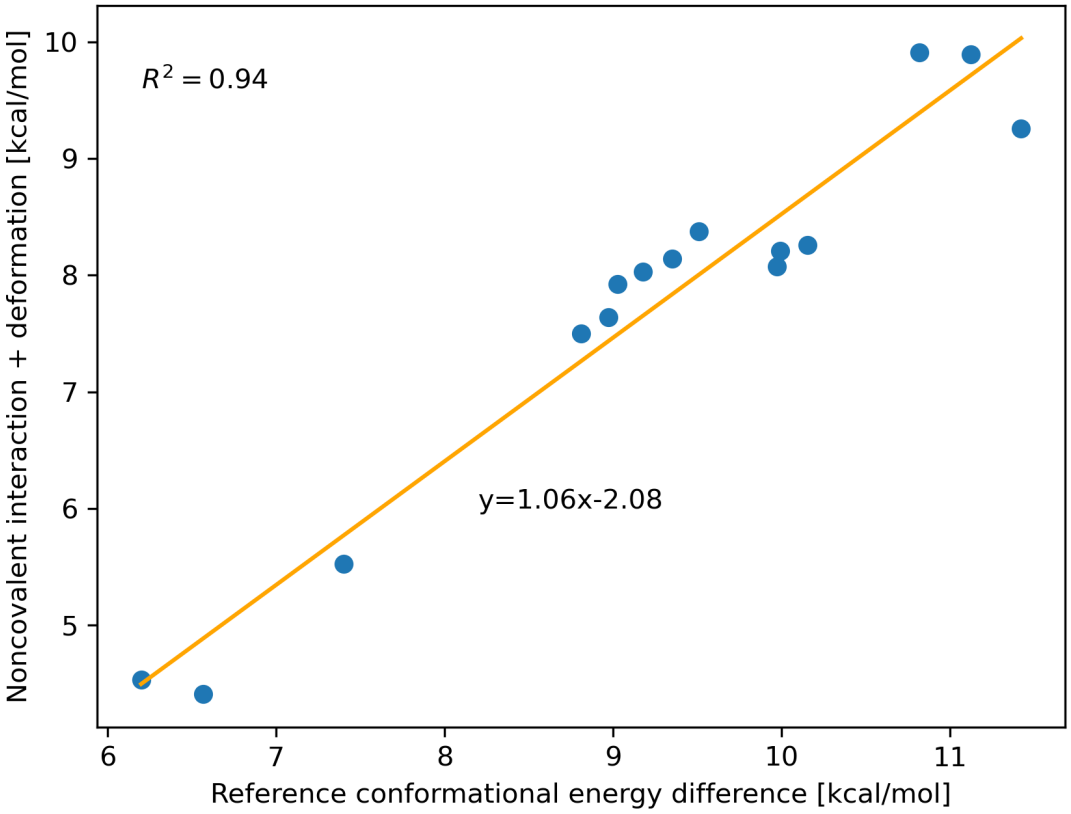

Figure 10: Correlation between the reference DLPNO-CCSD(T) conformational (cis–trans) energy difference and the sum of the ISAPT/SIAO1 intramolecular interaction energy difference and the deformation effect computed as the $\delta E_{\mathrm{def},1}$(XABY) quantity in Eq. (5). The orange line, with its formula shown on the graph, represents the best linear fir to the 15 energy differences for different substituent combinations.

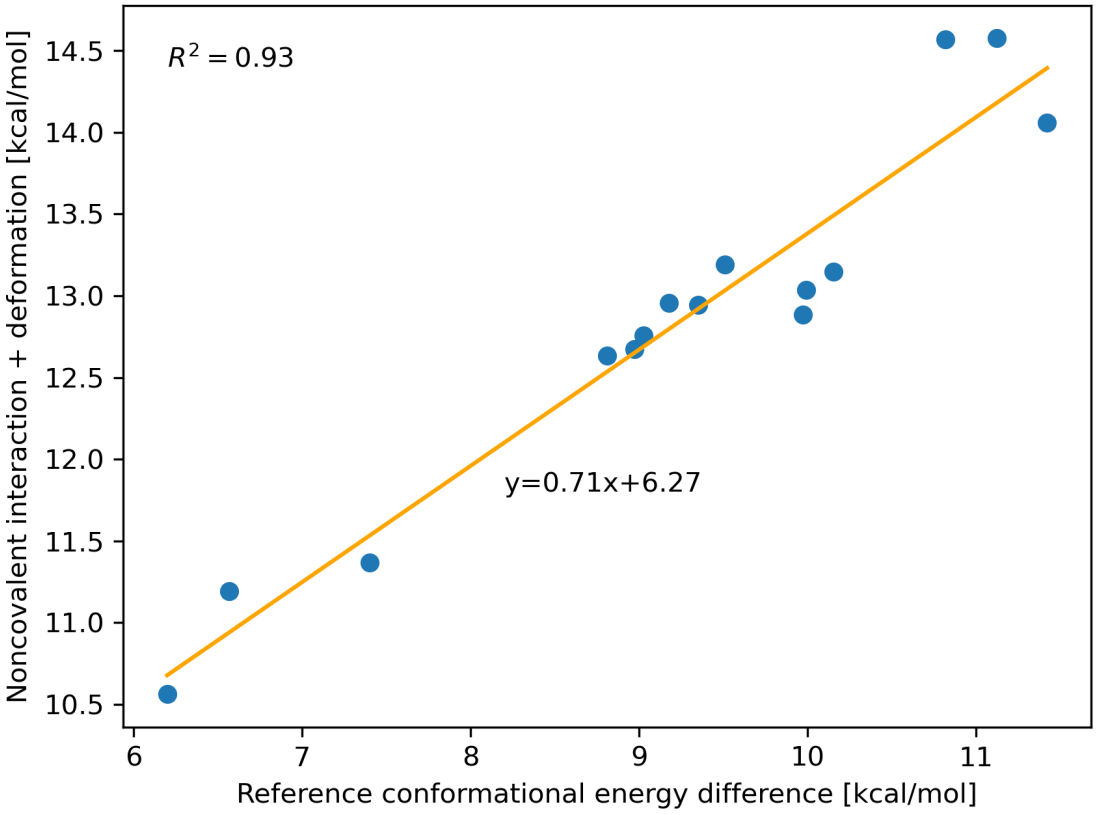

Figure 11: Correlation between the reference DLPNO-CCSD(T) conformational (cis–trans) energy difference and the sum of the ISAPT/SIAO1 intramolecular interaction energy difference and the deformation effect computed as the $\delta E_{\mathrm{def},2}$(XABY) quantity in Eq. (6). The orange line, with its formula shown on the graph, represents the best linear fir to the 15 energy differences for different substituent combinations.

Conclusions

The relative stability of the cis and trans conformations of substituted azobenzene is a net result of the molecular deformation that favors the flat, conjugated trans structure and the intramolecular noncovalent attraction, most notably London dispersion, that favors the closer inter-ring spacing of the cis structure. The latter interaction can be enhanced by aliphatic substituents acting as dispersion energy donors. Here, we perform accurate ab initio calculations to explain the interaction-deformation balance in 15 substituted azobenzenes in their optimized cis and trans structures. The noncovalent interaction energy is computed from a new ISAPT(SIAO1) variant of the intramolecular SAPT approach, and further decomposed into both physical contributions (electrostatics, induction, dispersion, and exchange) and the ring-ring, substituent-ring, and substituent-substituent terms. The deformation effect is estimated by computing energy differences for auxiliary one-ring systems that preserve molecular deformation as closely as possible but forgo the intramolecular nonbonded interaction. The sum of the two effects is compared to the conformational energy difference from reference DLPNO-CCSD(T) calculations.

We observed that, while the incorporation of substituents up to the *tert*-butyl size cannot make the cis structure more energetically favorable, it does make a substantial step in that direction: the DLPNO-CCSD(T)/aTZ cis-trans difference decreases from 11.4 kcal/mol in the unsubstituted AB system to 6.2 kcal/mol in the most substituted *t*BuAB*t*Bu one. This difference is due to the enhanced intramolecular interaction in the cis structure, a "steric attraction"; the ISAPT(SIAO1) calculations demonstrate that this attraction is primarily due to the enhanced dispersion interaction, followed by a secondary electrostatic effect. In contrast, the ISAPT(SIAO1) interaction energies for the trans structures show only a minor dependence on the substituent, and the intramolecular attraction is dominated by electrostatics in this case. A further decomposition of ISAPT data into fragment-fragment contributions within the F-ISAPT difference analysis framework allows us to directly analyze the substituent effects on the intramolecular interaction relative to unsubstituted azobenzene. In

the trans configurations, all ISAPT energy components are dominated by the indirect effects, that is, the alteration of the ring-ring interaction upon substitution. In contrast, for the cis systems only the first-order exchange is primarily indirect while the most favorable dispersion and electrostatic contributions are dominated by direct interactions involving at least one substituent. Finally, the two proposed schemes of estimating the deformation energy, when combined with the ISAPT intramolecular interaction energy data, show a very good linear correlation with the reference DLPNO-CCSD(T) conformational energy differences, showing that the energetic cis-trans balance can indeed be explained by a combination of nonbonded interaction and molecular deformation.

Acknowledgments

This work was supported by the U.S. National Science Foundation award CHE-1955328.

References

(1) Eisenschitz, R.; London, F. Über das Verhältnis der van der Waalsschen Kräfte zu den homöopolaren Bindungskräften. *Z. Phys.* **1930**, *60*, 491–527.

(2) Jeziorski, B.; Szalewicz, K.; Chałasiński, G. Symmetry Forcing and Convergence Properties of Perturbation Expansions for Molecular Interaction Energies. *Int. J. Quantum Chem.* **1978**, *14*, 271–287.

(3) Jeziorski, B.; Kołos, W. Symmetry forcing in perturbation theory of weak intermolecular interactions. *Int. J. Quantum Chem., Suppl. 1* **1977**, *12*, 91–117.

(4) Ćwiok, T.; Jeziorski, B.; Kołos, W.; Moszyński, R.; Szalewicz, K. On the Convergence of the Symmetrized Rayleigh-Schrödinger Perturbation Theory for Molecular Interaction Energies. *J. Chem. Phys.* **1992**, *97*, 7555–7559.

(5) Korona, T.; Moszyński, R.; Jeziorski, B. Convergence of symmetry-adapted perturbation theory for the interaction between helium atoms and between a hydrogen molecule and a helium atom. *Adv. Quantum Chem.* **1997**, *28*, 171–188.

(6) Patkowski, K.; Korona, T.; Jeziorski, B. Convergence behavior of the symmetry-adapted perturbation theory for states submerged in Pauli forbidden continuum. *J. Chem. Phys.* **2001**, *115*, 1137–1152.

(7) Rybak, S.; Jeziorski, B.; Szalewicz, K. Many-body symmetry-adapted perturbation theory of intermolecular interactions - H_2O and HF dimers. *J. Chem. Phys.* **1991**, *95*, 6579–6601.

(8) Moszyński, R.; Jeziorski, B.; Ratkiewicz, A.; Rybak, S. Many-body perturbation theory of electrostatic interactions between molecules: Comparison with full configuration interaction for four-electron dimers. *J. Chem. Phys.* **1993**, *99*, 8856–8869.

(9) Moszyński, R.; Jeziorski, B.; Rybak, S.; Szalewicz, K.; Williams, H. L. Many-body theory of exchange effects in intermolecular interactions. Density matrix approach and applications to He-F^-, He-HF, H_2-HF, and Ar-H_2 dimers. *J. Chem. Phys.* **1994**, *100*, 5080–5093.

(10) Misquitta, A. J.; Jeziorski, B.; Szalewicz, K. Dispersion energy from density-functional theory description of monomers. *Phys. Rev. Lett.* **2003**, *91*, 033201.

(11) Misquitta, A. J.; Podeszwa, R.; Jeziorski, B.; Szalewicz, K. Intermolecular potentials based on symmetry-adapted perturbation theory including dispersion energies from time-dependent density functional calculations. *J. Chem. Phys.* **2005**, *123*, 214103.

(12) Korona, T.; Moszyński, R.; Jeziorski, B. Electrostatic interactions between molecules from relaxed one-electron density matrices of the coupled cluster singles and doubles model. *Mol. Phys.* **2002**, *100*, 1723–1734.

(13) Korona, T.; Jeziorski, B. Dispersion energy from density-fitted density susceptibilities of singles and doubles coupled cluster theory. *J. Chem. Phys.* **2008**, *128*, 144107.

(14) Jeziorski, B.; van Hemert, M. C. Variation-perturbation treatment of the hydrogen bond between water molecules. *Mol. Phys.* **1976**, *31*, 713–729.

(15) Szalewicz, K.; Jeziorski, B. Symmetry-adapted double-perturbation analysis of intramolecular correlation effects in weak intermolecular interactions: the He-He interaction. *Mol. Phys.* **1979**, *38*, 191–208.

(16) Przybytek, M. Dispersion Energy of Symmetry-Adapted Perturbation Theory from the Explicitly Correlated F12 Approach. *J. Chem. Theory Comput.* **2018**, *14*, 5105–5117.

(17) Kodrycka, M.; Holzer, C.; Klopper, W.; Patkowski, K. Explicitly correlated dispersion and exchange dispersion energies in symmetry-adapted perturbation theory. *J. Chem. Theory Comput.* **2019**, *15*, 5965–5986.

(18) Kodrycka, M.; Patkowski, K. Efficient Density-Fitted Explicitly Correlated Dispersion and Exchange Dispersion Energies. *J. Chem. Theory Comput.* **2021**, *17*, 1435–1456.

(19) Piszczatowski, K.; Łach, G.; Jeziorski, B. Direct calculation of interaction-induced molecular properties: An application to the relativistic mass-velocity and Darwin terms in the interaction energy of hydrogen atoms. *Phys. Rev. A* **2008**, *77*, 062514.

(20) Tyrcha, B.; Gupta, T.; Patkowski, K.; Żuchowski, P. S. Analytical Derivatives of Symmetry-Adapted Perturbation Theory Corrections for Interaction-Induced Properties. *J. Chem. Theory Comput.* **2025**, *21*, 4562–4578.

(21) Tyrcha, B.; Stachowiak, M.; Patkowski, K.; Żuchowski, P. S. Direct calculation of dipole moment surfaces through second-order symmetry-adapted perturbation theory for properties. arXiv:2611.07993, **2026**.

(22) Patkowski, K. Recent developments in symmetry-adapted perturbation theory. *WIREs Comput. Mol. Sci.* **2020**, *10*, e1452.

(23) Garcia, J.; Podeszwa, R.; Szalewicz, K. SAPT codes for calculations of intermolecular interaction energies. *J. Chem. Phys.* **2020**, *152*, 184109.

(24) Szalewicz, K.; Jeziorski, B. Physical mechanisms of intermolecular interactions from symmetry-adapted perturbation theory. *J. Mol. Model.* **2022**, *28*, 273.

(25) Korona, T.; Hapka, M.; Pernal, K.; Patkowski, K. In *Polish Quantum Chemistry from Kołos to Now*; Musiał, M., Grabowski, I., Eds.; Adv. Quantum Chem., 2023; Vol. 87; pp 37–72.

(26) Patkowski, K. Understanding nonbonded interactions between molecular fragments. *Chem. Commun.* **2026**, *62*, 419–432.

(27) Parrish, R. M.; Sherrill, C. D. Spatial assignment of symmetry adapted perturbation theory interaction energy components: The atomic SAPT partition. *J. Chem. Phys.* **2014**, *141*, 044115.

(28) Parrish, R. M.; Parker, T. M.; Sherrill, C. D. Chemical Assignment of Symmetry-Adapted Perturbation Theory Interaction Energy Components: The Functional-Group SAPT Partition. *J. Chem. Theory Comput.* **2014**, *10*, 4417–4431.

(29) Pastorczak, E.; Prlj, A.; Gonthier, J. F.; Corminboeuf, C. Intramolecular symmetry-adapted perturbation theory with a single-determinant wavefunction. *J. Chem. Phys.* **2015**, *143*, 224107.

(30) Parrish, R. M.; Gonthier, J. F.; Corminboeuf, C.; Sherrill, C. D. Communication: Practical intramolecular symmetry adapted perturbation theory via Hartree-Fock embedding. *J. Chem. Phys.* **2015**, *143*, 051103.

(31) Lotrich, V. F.; Szalewicz, K. Symmetry-adapted perturbation theory of three-body nonadditivity in Ar trimer. *J. Chem. Phys.* **1997**, *106*, 9688–9702.

(32) Podeszwa, R.; Szalewicz, K. Three-body symmetry-adapted perturbation theory based on Kohn-Sham description of the monomers. *J. Chem. Phys.* **2007**, *126*, 194101.

(33) Lao, K. U.; Herbert, J. M. Accurate and Efficient Quantum Chemistry Calculations for Noncovalent Interactions in Many-Body Systems: The XSAPT Family of Methods. *J. Phys. Chem. A* **2015**, *119*, 235–252.

(34) Sirianni, D. A.; Zhu, X.; Sitkoff, D. F.; Cheney, D. L.; Sherrill, C. D. The influence of a solvent environment on direct non-covalent interactions between two molecules: A symmetry-adapted perturbation theory study of polarization tuning of π-π interactions by water. *J. Chem. Phys.* **2022**, *156*, 194306.

(35) Glick, C. S.; Alenaizan, A.; Cheney, D. L.; Cavender, C. E.; Sherrill, C. D. Electrostatically embedded symmetry-adapted perturbation theory. *J. Chem. Phys.* **2024**, *161*, 134112.

(36) Meitei, O. R.; Hesselmann, A. On the Stability of Cyclophane Derivates Using a Molecular Fragmentation Method. *ChemPhysChem* **2016**, *17*, 3863–3874.

(37) Meitei, O. R.; Hesselmann, A. Intramolecular Interactions in Sterically Crowded Hydrocarbon Molecules. *J. Comput. Chem.* **2017**, *38*, 2500–2508.

(38) Gonthier, J. F.; Corminboeuf, C. Exploration of zeroth-order wavefunctions and energies as a first step toward intramolecular symmetry-adapted perturbation theory. *J. Chem. Phys.* **2014**, *140*, 154107.

(39) Mayer, I. Towards a "Chemical" Hamiltonian. *Int. J. Quantum Chem.* **1983**, *23*, 341–363.

(40) Manby, F. R.; Stella, M.; Goodpaster, J. D.; Miller III, T. F. A Simple, Exact Density-Functional-Theory Embedding Scheme. *J. Chem. Theory Comput.* **2012**, *8*, 2564–2568.

(41) Parker, T. M.; Burns, L. A.; Parrish, R. M.; Ryno, A. G.; Sherrill, C. D. Levels of Symmetry Adapted Perturbation Theory (SAPT). I. Efficiency and Performance for Interaction Energies. *J. Chem. Phys.* **2014**, *140*, 094106.

(42) Knizia, G. Intrinsic Atomic Orbitals: An Unbiased Bridge between Quantum Theory and Chemical Concepts. *J. Chem. Theory Comput.* **2013**, *9*, 4834–4843.

(43) Luu, D.; Patkowski, K. Overcoming Artificial Multipoles in Intramolecular Symmetry-Adapted Perturbation Theory. *J. Phys. Chem. A* **2023**, *127*, 356–377.

(44) Luu, D.; Corminboeuf, C.; Patkowski, K. Range Separation of the Interaction Potential in Intermolecular and Intramolecular Symmetry-Adapted Perturbation Theory. *J. Chem. Theory Comput.* **2024**, *20*, 7884–7903.

(45) Lednev, I. K.; Ye, T.-Q.; Hester, R. E.; Moore, J. N. Femtosecond Time-Resolved UV-Visible Absorption Spectroscopy of trans-Azobenzene in Solution. *J. Phys. Chem.* **1996**, *100*, 13338.

(46) Fujino, T.; Arzhantsev, S. Y.; Tahara, T. Femtosecond Time-Resolved Fluorescence Study of Photoisomerization of trans-Azobenzene. *J. Phys. Chem. A* **2001**, *105*, 8123–8129.

(47) Lednev, K.; Ye, T.-Q.; Matousek, P.; Towrie, M.; Foggi, P.; Neuwahl, F.; Umapathy, S.; Hester, R.; Moore, J. N. Femtosecond time-resolved UV-visible absorption spectroscopy of trans-azobenzene: dependence on excitation wavelength. *Chem. Phys. Lett.* **1998**, *290*, 68–74.

(48) Mahimwalla, Z.; Yager, K. G.; Mamiya, J.; Shishido, A.; Priimagi, A.; Barrett, C. J.

Azobenzene photomechanics: prospects and potential applications. *Polym. Bull.* **2012**, *69*, 967–1006.

(49) Chang, C.-W.; Lu, Y.-C.; Wang, T.-T.; Diau, E. W.-G. Photoisomerization Dynamics of Azobenzene in Solution with S1 Excitation: A Femtosecond Fluorescence Anisotropy Study. *J. Am. Chem. Soc.* **2004**, *126*, 10109–10118.

(50) Schultz, T.; Quenneville, J.; Levine, B.; Toniolo, A.; Mart´ınez, T. J.; Lochbrunner, S.; Schmitt, M.; Schaffer, J. P.; Zgierski, M. Z.; Stolow, A. Mechanism and dynamics of azobenzene photoisomerization. *J. Am. Chem. Soc.* **2003**, *125*, 8098–8099.

(51) Bandara, H. M. D.; Burdette, S. C. Photoisomerization in different classes of azobenzene. *Chem. Soc. Rev.* **2012**, *41*, 1809–1825.

(52) Cembran, A.; Bernardi, F.; Garavelli, M.; Gagliardi, L.; Orlandi, G. On the Mechanism of the cis-trans Isomerization in the Lowest Electronic States of Azobenzene: S0, S1, and T1. *J. Am. Chem. Soc.* **2004**, *126*, 3234–3243.

(53) Cojocariu, C.; Rochon, P. Light-induced motions in azobenzene-containing polymers. *Pure Appl. Chem.* **2004**, *76*, 1479–1497.

(54) Cusati, T.; Granucci, G.; Persico, M. Photodynamics and Time-Resolved Fluorescence of Azobenzene in Solution: A Mixed Quantum-Classical Simulation. *J. Am. Chem. Soc.* **2011**, *133*, 5109–5123.

(55) Shipway, A. N.; Willner, I. Electronically transduced molecular mechanical and information functions on surfaces. *Acc. Chem. Res.* **2001**, *34*, 421–432.

(56) Ballardini, R.; Balzani, V.; Credi, A.; Gandolfi, M. T.; Venturi, M. Artificial molecular-level machines: which energy to make them work? *Acc. Chem. Res.* **2001**, *34*, 445–455.

(57) Dugave, C.; Demange, L. Cis-Trans Isomerization of Organic Molecules and Biomolecules: Implications and Applications. *Chem. Rev.* **2003**, *103*, 2475–2532.

(58) Klajn, R. Immobilized azobenzenes for the construction of photoresponsive materials. *Pure Appl. Chem.* **2010**, *82*, 2247–2279.

(59) Yager, K. G.; Barrett, C. J. Novel photo-switching using azobenzene functional materials. *Journal of Photochemistry and Photobiology A: Chemistry* **2006**, *182*, 250–261.

(60) Ercole, F.; Davis, T. P.; ; Evans, R. A. Photo-responsive systems and biomaterials: photochromic polymers, light-triggered self-assembly, surface modification, fluorescence modulation and beyond. *Polym. Chem.* **2010**, *1*, 37–54.

(61) Wang, Y.; Huang, L.; Wang, X.; Lu, X.; Wang, B.; Qin, Y.; Huang, C. Photoresponsive triple shape memory polymers with a self-healing function based on poly (lactic acid)/polycaprolactone blends. *Polymer Testing* **2023**, *120*, 107966.

(62) Zheng, M.; Yuan, J. Polymeric nanostructures based on azobenzene and their biomedical applications: synthesis, self-assembly and stimuli-responsiveness. *Org. Biomol. Chem.* **2022**, *20*, 749–767.

(63) García-Amorós, J.; Velasco, D. Recent advances towards azobenzene-based light-driven real-time information-transmitting materials. *Beilstein J. Org. Chem.* **2012**, *8*, 1003–1017.

(64) Jacquemin, D.; Preat, J.; Perpète, E. A.; Vercauteren, D. P.; André, J.; Ciofini, I.; Adamo, C. Absorption Spectra of Azobenzenes Simulated With Time-Dependent Density Functional Theory. *Int. J. Quantum Chem.* **2011**, *111*, 4224–4240.

(65) Fliegl, H.; Köhn, A.; Hättig, C.; Ahlrichs, R. Ab Initio Calculation of the Vibrational and Electronic Spectra of trans- and cis-Azobenzene. *J. Am. Chem. Soc.* **2003**, *125*, 9821–9827.

(66) Dubecký, M.; Derian, R.; Mitas, L.; Štich, I. Ground and excited electronic states of azobenzene: A quantum Monte Carlo study. *J. Chem. Phys.* **2010**, *133*, 244301.

(67) Hutcheson, A.; Paul, A. C.; Myhre, R. H.; Koch, H.; Høyvik, I. Describing ground and excited state potential energy surfaces for molecular photoswitches using coupled cluster models. *J. Comput. Chem.* **2021**, *42*, 1419–1429.

(68) Riplinger, C.; Neese, F. An efficient and near linear scaling pair natural orbital based local coupled cluster method. *J. Chem. Phys.* **2013**, *138*, 034106.

(69) Riplinger, C.; Sandhoefer, B.; Hansen, A.; Neese, F. Natural Triple Excitations in Local Coupled Cluster Calculations with Pair Natural Orbitals. *J. Chem. Phys.* **2013**, *139*, 134101.

(70) Guo, Y.; Riplinger, C.; Becker, U.; Liakos, D. G.; Minenkov, Y.; Cavallo, L.; Neese, F. Communication: An improved linear scaling perturbative triples correction for the domain based local pair-natural orbital based singles and doubles coupled cluster method [DLPNO-CCSD(T)]. *J. Chem. Phys.* **2018**, *148*, 011101.

(71) Smith, D. G. A.; Burns, L. A.; Simmonett, A. C.; Parrish, R. M.; Schieber, M. C.; Galvelis, R.; Kraus, P.; Kruse, H.; Di Remigio, R.; Alenaizan, A. et al. Psi4 1.4: Open-source software for high-throughput quantum chemistry. *J. Chem. Phys.* **2020**, *152*, 184108.

(72) Parrish, R. M.; Sherrill, C. D. Quantum-Mechanical Evaluation of π-π versus Substituent-π Interactions in π Stacking: Direct Evidence for the Wheeler-Houk Picture. *J. Am. Chem. Soc.* **2014**, *136*, 17386–17389.

(73) Di Berardino, C.; Strauss, M. A.; Schatz, D.; Wegner, H. A. An Incremental System To Predict the Effect of Different London Dispersion Donors in All-meta-Substituted Azobenzenes. *Chem. Eur. J.* **2022**, *28*, e202104284.

(74) Grimme, S.; Ehrlich, S.; Goerigk, L. Effect of the Damping Function in Dispersion Corrected Density Functional Theory. *J. Comput. Chem.* **2011**, *32*, 1456–1465.

(75) Řezáč, J.; Hobza, P. Benchmark Calculations of Interaction Energies in Noncovalent Complexes and Their Applications. *Chem. Rev.* **2016**, *116*, 5038–5071.

(76) Frisch, M. J.; Trucks, G. W.; Schlegel, H. B.; Scuseria, G. E.; Robb, M. A.; Cheeseman, J. R.; Scalmani, G.; Barone, V.; Petersson, G. A.; Nakatsuji, H. et al. Gaussian 16, Revision B.01. Gaussian, Inc., Wallingford, CT, 2016.

(77) Neese, F. Software Update: The ORCA Program System—Version 6.0. *Wiley Interdiscip. Rev. Comput. Mol. Sci.* **2025**, *15*, e70019.

(78) Jeziorski, B.; Moszyński, R.; Szalewicz, K. Perturbation Theory Approach to Intermolecular Potential Energy Surfaces of van der Waals Complexes. *Chem. Rev.* **1994**, *94*, 1887–1930.

(79) Hemmati, R.; Patkowski, K. Ab Initio Study of Chiral Discrimination in the Glycidol Dimer. *J. Phys. Chem. A* **2020**, *124*, 9436–9450.

Supplementary Files

This is a list of supplementary files associated with this preprint. Click to download.

- SI.pdf
- optimizedstructures.zip